COMPDYN 2013
4th ECCOMAS Thematic Conference on
Computational Methods in Structural Dynamics and Earthquake Engineering
M. Papadrakakis, N.D.Lagaros, V. Plevris (eds.)
Kos Island, Greece, 12–14 June 2013

STOCHASTIC RESPONSE DETERMINATION AND RELIABILITY ASSESSMENT OF A NONLINEAR CABLE NET STRUCTURAL SYSTEM

Ioannis A. Kougioumtzoglou[1], Isabella Vassilopoulou[2] and Charis J. Gantes[2]

[1] Institute for Risk & Uncertainty, University of Liverpool
Brodie Tower, Brownlow Street, L69 3GQ, Liverpool, United Kingdom
kougioum@liverpool.ac.uk

[2] Institute of Steel Structures, School of Engineering, National Technical University of Athens
9, Iroon Polytechniou Street, GR-15780 Zografou, Athens, Greece
isabella@central.ntua.gr; chgantes@central.ntua.gr

Keywords: Cable Net, Nonlinear System, Dimension Reduction, Random Vibration, Reliability Assessment, Uncertainty Quantification.

Abstract. *A multi-degree-of-freedom (MDOF) symmetric cable net system with fixed cable ends under Gaussian white noise excitation is considered. First, a dimension reduction approach based on similarity relations is employed to cast the original MDOF system into an equivalent single-degree-of-freedom (SDOF) nonlinear oscillator of the hardening Duffing kind. Next, a numerical path integral (NPI) approach is utilized for determining the reduced system non-stationary response amplitude probability density function (PDF). The main concept of the approach relates to the evolution of the response PDF in short time steps, assuming a Gaussian form for the conditional response PDF. Further, the NPI approach is employed for determining first-passage kind reliability statistics of the Duffing oscillator; these are associated with the probability of cable tensile failure for specific mechanical and geometrical characteristics of the original cable net system. It is noted that the main advantages of the approximate deterministic approach of dimension reduction relate to a) the detection of nonlinear phenomena, such as the occurrence of sub/super-harmonic resonances, jump phenomena, etc, and b) the reduction of the computational effort associated with the nonlinear dynamic analysis of the original MDOF system. The latter advantage becomes significantly more important in the case of stochastic excitation where Monte Carlo simulation (MCS) methodologies can be computationally prohibitive, especially for cases of large scale complex systems. Hopefully, the herein developed approximate stochastic approach can be used as a convenient tool for preliminary reliability based design of the original MDOF structural system.*

1 INTRODUCTION

In 1953, when the first saddle-form cable net was studied and constructed, covering the Raleigh Arena in North Carolina, USA, a new era begun for such tensile structures. Since then, many similar structures have been used as roofs to large span facilities. Their shape is characterized by two opposite curvatures, defined by their sags, realized by two families of prestressed cables, the carrying and the stabilizing ones, which create an orthogonal net. They are called tensile structures because only tension can develop in their elements. Any local slackening of cables may lead to a total failure of the structure, thus their design is focused on ensuring a minimum tension in cables, under any loading combination.

Their behaviour is strongly nonlinear, exhibiting large displacements when they are loaded, leading to a significant change of their stiffness as the deformation evolves. This means that the internal forces do not vary linearly with the applied load. Their static analysis is based on iterative methods calculating the deformed geometry and the stiffness of the system for every load step. Their dynamic response instead, is much more complex due to particular nonlinear dynamic phenomena that may occur [1].

In [2] a preliminary design method was proposed by two of the authors of this paper for estimating the nonlinear dynamic response of a MDOF cable net using the analytical solution of an equivalent SDOF model. Nonlinear dynamic phenomena, such as bending of the response curve, jump phenomena, secondary resonances and dependence of the steady state response on the initial conditions, easily detected by solving analytically the equation of motion of the SDOF model, were verified for the MDOF system with surprising accuracy. This method was the evolution of a work first presented by Gero ([3], [4]) aiming at estimating the static behaviour of a large cable net with fixed cable ends using the response of a smaller similar system. The method was extended by the present authors to elastically supported cable network structures ([5] – [7]), proceeding later to the dynamic response of the net for the case of fixed cable ends [8].

In this paper a further step is achieved towards the design of such systems. In the traces of the previously presented preliminary design method, this investigation focuses on determining the non-stationary stochastic dynamic response and on assessing the reliability of such systems subjected to white noise excitation. In this regard, a numerical path integral (NPI) solution approach, recently proposed by the first author [9], is applied to the reduced SDOF nonlinear system for determining the non-stationary response probability density function (PDF) as well as the reliability function (survival probability). Specifically, based on the concepts of statistical linearization and of stochastic averaging the system response amplitude is modelled as a one-dimensional Markov diffusion process. Further, using a discrete version of the Chapman-Kolmogorov (C-K) equation and the associated first-order stochastic differential equation (SDE), the response amplitude PDF and the corresponding reliability function are derived. The main concept of the approach relates to the evolution of the response PDF in short time steps, assuming a Gaussian form for the conditional response PDF.

In this manner, the proposed methodology can be utilized for a preliminary reliability based design. In this regard, the mechanical and geometrical characteristics of the structure can be chosen appropriately to avoid large values of the cable tensile failure probability. The accuracy of the proposed method is illustrated by means of an illustrative example.

2 MODELLING ISSUES AND ASSUMPTIONS

Two different models are used in this paper. The first one is a multi-degree-of-freedom (MDOF) symmetric saddle-shaped cable net, called prototype and symbolized as ‘p’, while the second one is a SDOF cable net system, which is referred to as model, and denoted as ‘m’.

2.1 Prototype

The prototype has a circular plan view of diameter L_p and sag f_p, equal in both directions. It consists of N_p cables in each direction, arranged in a quadratic grid (Figure 1). Both groups of cables have a circular cross-section with area A_p, while their material is assumed to be linearly elastic with Young modulus E_p in tension and zero compression branch. The maximum cable stress is assumed equal to the yield stress of the material σ_y, corresponding to a strain $\varepsilon_{max}=\sigma_y/E_p$. The net is uniformly prestressed, considering an initial cable elongation $\varepsilon_p=(N_0)_p/(E_pA_p)$ equal for all cables, where $(N_0)_p$ is the initial pretension. The cable mass density is m_p. A lumped mass matrix is taken into account, thus the distributed mass along the length of the cables is concentrated at the nodes. A Rayleigh damping [10] is also assumed, taking into account a damping ratio ζ_p. All cables are modelled as straight truss elements between two adjacent intersection points. Equal concentrated dynamic loads, defined as $P_p(t)$, are exerted vertically on all nodes of the net, having the same amplitude and time variation. The three translational degrees of freedom are considered as free for all internal nodes of the net, while the cable ends are assumed as pinned. All analyses for the MDOF model are performed with the finite element software ADINA ([11], [12]) considering the geometry and stiffness of the state under pretension; thus, no form-finding analysis is carried out. The error introduced by this assumption is negligible as proved in [1]. The response of the system is represented by the vertical displacement of the central node located at the origins of the axes, where the maximum oscillation amplitude is observed.

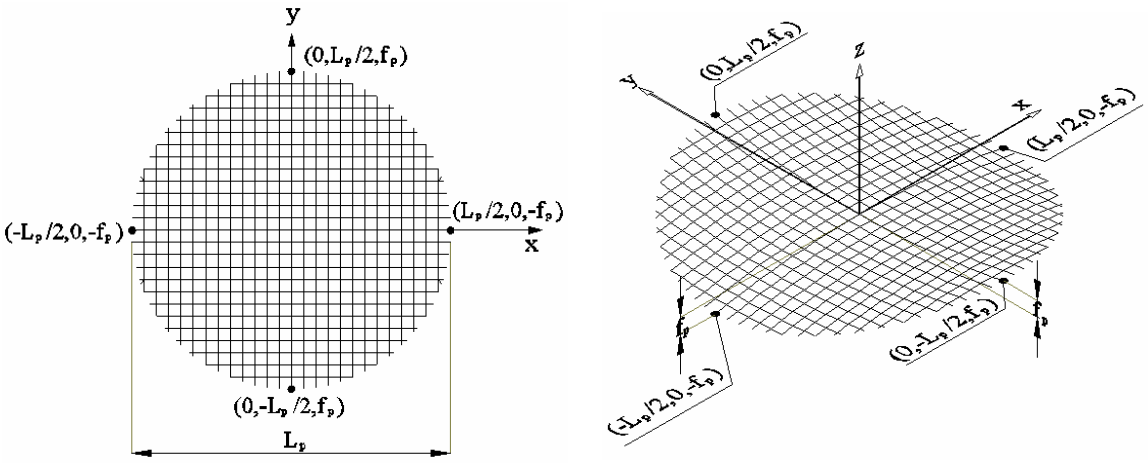

(a) (b)

Figure 1: Geometry of the MDOF cable net (prototype) (a) plan view, (b) perspective view

2.2 Model

The model is the simplest possible cable net system, consisting of two perpendicularly crossing cables, intersecting at their mid-spans. Thus, four straight cable elements are formed between the external nodes and the central one (Figure 2). Both cables have the same initial pretension $(N_0)_m$, material with elastic modulus E_m, cross-sectional area A_m, equal lengths L_m and equal but opposite sags f_m. The damping ratio of the system is ζ_m. The central node is free, while the ends of the cables are fixed. A concentrated mass M_m and a vertical dynamic load $P_m(t)$ are applied on the central node. Due to the symmetry of the structure, the only degree of freedom is the vertical displacement of the central node. As in the case of the prototype, the vertical displacement of the central node represents the response of the model.

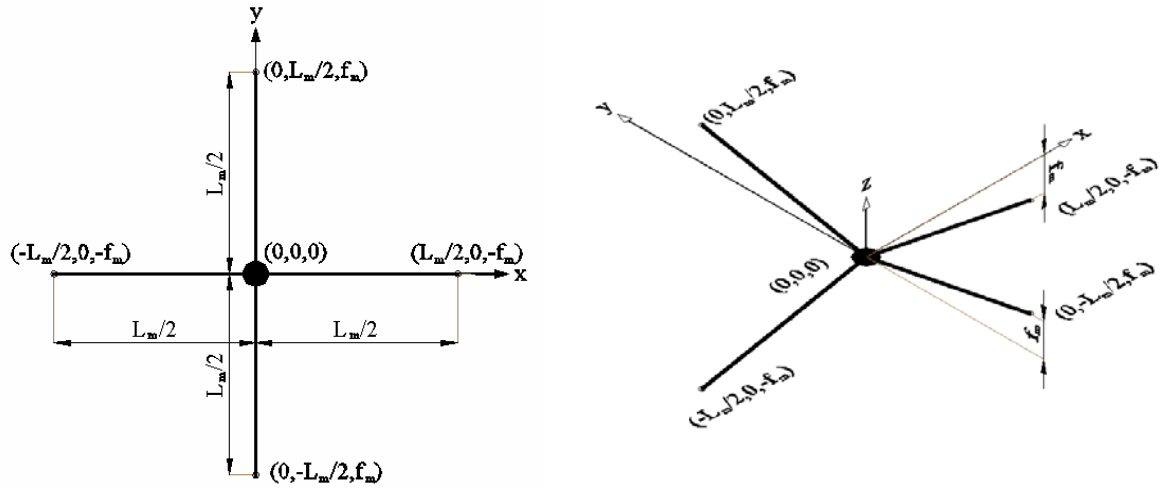

(a) (b)

Figure 2: Geometry of the SDOF cable net (model) (a) plan view, (b) perspective view

As demonstrated in [13], the SDOF model can be simulated with great accuracy by a hardening Duffing oscillator [14], given by the following equation of motion:

$$\ddot{x} + 2\zeta\omega_m\dot{x} + \omega_m^2 x + \frac{16E_mA_m}{M_mL_m^3}x^3 = \frac{P_m(t)}{M_m} = w(t) \tag{1}$$

where x represents the vertical displacement of the central node, while its first and second derivatives are the corresponding velocity and acceleration, respectively. The eigenfrequency of the system is expressed as:

$$\omega_m = \sqrt{\frac{4E_mA_m}{M_mL_m}\cdot\left(8\frac{f_m^2}{L_m^2} + 2\frac{(N_0)_m}{E_mA_m} - 4\frac{(N_0)_m}{E_mA_m}\frac{f_m^2}{L_m^2}\right)} \tag{2}$$

3 DIMENSION REDUCTION METHOD

The dimension reduction method is based on the transformation of a large cable net (prototype) into a smaller cable net (model), using similarity relations which include the geometric and mechanical characteristics of both systems.

3.1 Similarity relations

The relations used in this paper are based on the ones provided in [2] and are the following:

$$(P_0)_m = (P_0)_p\left(\frac{E_m}{E_p}\right)\left(\frac{L_m}{L_p}\right)^2\left(\frac{N_p+1}{N_m+1}\right)^2\sqrt{\frac{f_m/L_m}{f_p/L_p}}\text{ : load amplitude} \tag{3}$$

$$D_m = D_p\left(\frac{L_m}{L_p}\right)\sqrt{\left(\frac{N_p+1}{N_m+1}\right)\left(\frac{f_p/L_p}{f_m/L_m}\right)}\text{ : cable diameter} \tag{4}$$

$$A_m = A_p\left(\frac{L_m}{L_p}\right)^2\left(\frac{N_p+1}{N_m+1}\right)\left(\frac{f_p/L_p}{f_m/L_m}\right)^2 : \text{cable cross-sectional area} \quad (5)$$

$$(EA)_m = (EA)_p\left(\frac{E_m}{E_p}\right)\left(\frac{L_m}{L_p}\right)^2\left(\frac{N_p+1}{N_m+1}\right)\left(\frac{f_p/L_p}{f_m/L_m}\right)^2 : \text{axial stiffness} \quad (6)$$

$$(N_0)_m = (N_0)_p\left(\frac{E_m}{E_p}\right)\left(\frac{L_m}{L_p}\right)^2\left(\frac{N_p+1}{N_m+1}\right) : \text{initial pretension} \quad (7)$$

$$M_m = M_p\left(\frac{E_m}{E_p}\right)\left(\frac{L_m}{L_p}\right)\left(\frac{N_p+1}{N_m+1}\right)^2 : \text{nodal mass} \quad (8)$$

$$x_{d,m} = x_{d,p}\left(\frac{L_m}{L_p}\right)\left(\frac{f_m/L_m}{f_p/L_p}\right) : \text{nodal dynamic deflection} \quad (9)$$

$$\Omega_m=\Omega_p : \text{loading frequency} \quad (10)$$

where N is the number of cables in each direction, while the subscripts m and p stand for model and prototype, respectively.

Potential discrepancies of the results extracted by this method decrease as the similarities between the two systems increase. In order to minimized the error introduced by the dimension reduction, the cable span, the sag and the elastic modulus of the material are chosen to be equal for both prototype and model, thus, $L_m=L_p$, $f_m=f_p$ and $E_m=E_p$.

3.2 Example

The MDOF cable net is the one described in [2] and also studied in [1]. It has a diameter L_p=100m and a sag-to-span ratio equal to f_p/L_p=1/35 (f_p=2.857m), while the number of cables in each direction is N_p=25. The cable diameter is D_p=50mm with cross-sectional area A_p=0.00196m^2. The Young modulus is E_p=165GPa. The pretension is $(N_0)_p$=600kN, corresponding to approximately 20% of the yield stress, which is considered equal to 1570MPa, considering one of the two most common categories of steel for cables, 1570/1770MPa. Assuming that cable failure occurs when the cable stress becomes equal to the yield stress, the maximum permissible cable tension is:

$$(N_c)_{max,p}=A_p\sigma_y=0.00196\text{m}^2\cdot 157000\text{kN/m}^2=3082\text{kN} \quad (11)$$

corresponding to a strain of cables ε_{max}=0.0095. Thus, the material constitutive law taken into account for all analyses of the prototype is illustrated in Figure 3.

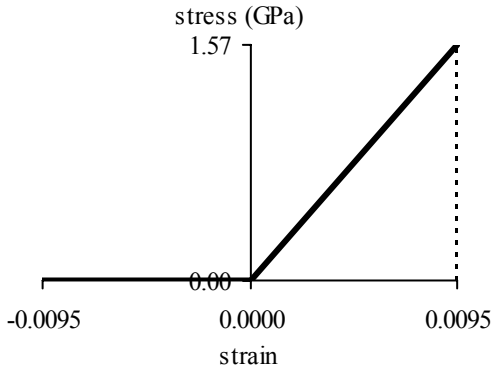

Figure 3: Material constitutive law

The unit weight of the cables is taken equal to ρ_p=100kN/m^3, which corresponds to a concentrated mass on every node equal to:

$$M_p = \frac{2A_p\rho_p L_p}{g(N_p+1)} = 0.151\text{kN}\,\text{sec}^2\,\text{m}^{-1} \tag{12}$$

where g=10m/sec^2. In this work a damping ratio equal to ζ_p=2% is assumed, a common value for such structures, as mentioned in [15]. Performing modal analysis the eigenmodes and eigenfrequencies are calculated. The first six are shown in Figure 4. The first vibration mode is the first symmetric mode having frequency ω_p=9.902sec^{-1}. In this paper this is considered as the main vibration mode.

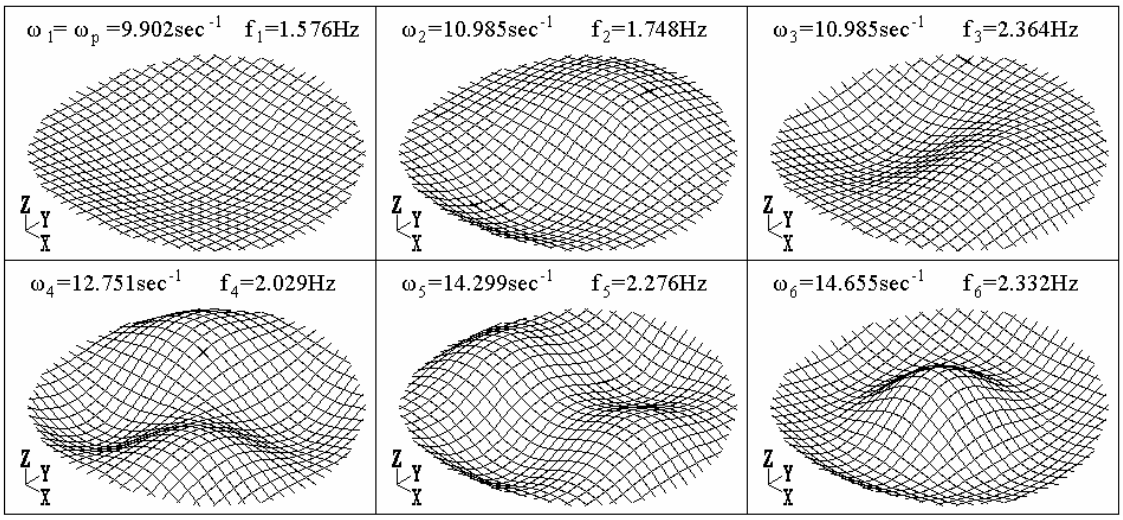

Figure 4: The first six vibration modes of the prototype

Taking into account that for the model N_m=1 cable in each direction, L_m=L_p=100m, f_m/L_m= f_p/L_p=1/35 (f_m=2.857m), and E_m=E_p=165GPa, based on the similarity relations, the equivalent SDOF model has the following characteristics:

$$A_m = A_p\left(\frac{N_p+1}{N_m+1}\right) = 0.00196\cdot\frac{26}{2} = 0.0255\text{m}^2 \tag{13}$$

$$(N_0)_m = (N_0)_p \left(\frac{N_p + 1}{N_m + 1} \right) = 600 \frac{26}{2} = 7800\text{kN} \tag{14}$$

$$M_m = M_p \left(\frac{N_p + 1}{N_m + 1} \right)^2 = 0.151 \cdot \left(\frac{26}{2} \right)^2 = 25.52\text{kN}\,\text{sec}^2\,\text{m}^{-1} \tag{15}$$

In the case of the model the maximum cable tension is:

$$(N_c)_{,max,m} = A_m \sigma_y = 0.0255\text{m}^2 \cdot 157000\text{kN/m}^2 = 40035\text{kN} \tag{16}$$

and the maximum permissible deflection is equal 3.975m, as calculated in [1]. Due to its geometry, the maximum vertical displacement of the central node corresponds to the maximum cable stress.

One of the drawbacks of this method is that the analytical solution of the Duffing oscillator's equation of motion, expressed by Eq. (1), does not take into account an eventual slackening of the cables. This is not an issue in this investigation, as the level of pretension does not allow any cable slackening for any displacement. In Figure 5, where the cable tension is plotted for both cables up to the maximum deflection of the central node, it is noted that both cables remain always under tension.

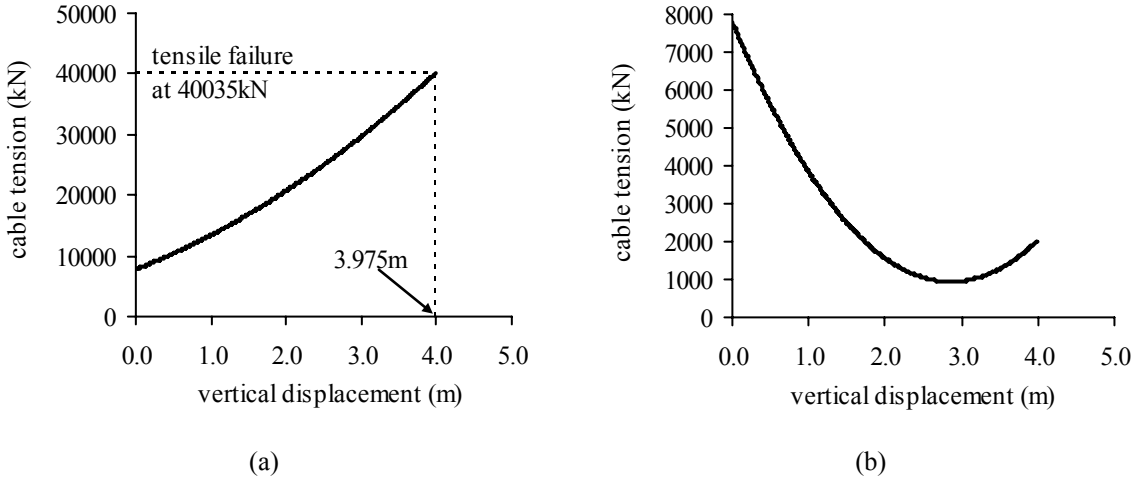

Figure 5: Cable tension diagrams with respect to the vertical displacement of the central node of the model: (a) Carrying cables (b) Stabilizing cables

3.3 Additional and improved similarity relations

For the purposes of the investigation presented in this paper, new transformations are added and some improvements in the similarity relations used in previous works, are introduced. In [2], the interest of the authors was focused on the estimation of the steady-state response of the prototype; thus, the structural response behaviour of the transient phase was neglected. In this investigation it is suggested to scale also time, as it plays an important role in the non-stationary stochastic response determination and reliability assessment of the prototype. In this regard, considering the characteristics of the prototype, given in section 3.2, and using the similarity relations to transform them into the corresponding ones of the model, the response to a harmonic load is calculated and compared for both systems, performing nonlinear time-history analyses with ADINA for the MDOF system and solving the equation

of motion for the SDOF model with MATLAB [16]. In the following, zero damping is chosen for the analyses so that the resonance phenomenon is illustrated more clearly.

The natural frequency of the model is calculated according to Eq. (2) and it is equal to $\omega_m=8.22\text{sec}^{-1}$. The ratio ω_m/ω_p is 0.83 and it is equal to $[(N_m+1)/(N_p+1)]^{0.07}=(2/26)^{0.07}=0.83$. Thus, an improved similarity relation is proposed herein, with respect to the one given in [2], connecting the natural frequencies of the two systems, defined as:

$$\omega_m = \omega_p \left(\frac{N_m + 1}{N_p + 1} \right)^{0.07} \tag{17}$$

A harmonic load acts on every node of the prototype, described as $P_p(t)=(P_0)_p\cos\Omega_p t$, with amplitude $(P_0)_p=1\text{kN}$, which is transformed for the model according to relation (3):

$$(P_0)_m = (P_0)_p \left(\frac{N_p + 1}{N_m + 1} \right)^2 = 1 \cdot \left(\frac{26}{2} \right)^2 = 169\text{kN} \tag{18}$$

Three loading frequencies are chosen for the prototype $\Omega_p=0.33\omega_p$, $\Omega_p=\omega_p$ and $\Omega_p=1.2\omega_p$, while for the model they become $\Omega_m=0.33\omega_m$, $\Omega_m=\omega_m$ and $\Omega_m=1.2\omega_m$. The equation of motion of the undamped SDOF system, expressed by Eq. (1), becomes:

$$\ddot{x} + (8.22\,\text{sec}^{-1})^2 x + (2.64\,\text{sec}^{-2}\,\text{m}^{-2}) x^3 = (6.62\text{m}/\text{sec}^2)\cos\Omega_m t \tag{19}$$

In case of fundamental resonance without damping each system vibrates with a frequency equal to its eigenfrequency and consequently, the period of the response of each system is related to its natural frequency. Thus, a new similarity relation is generated to scale the time of the model's response in order to match the one of the prototype.

$$t_p = t_m \left(\frac{N_m + 1}{N_p + 1} \right)^{0.07} \tag{20}$$

Figure 6a shows the time history diagrams of the vertical displacement for both systems, as calculated without time transformation. It is concluded that it is necessary to scale time for the SDOF model in order to match the response of the prototype. In Figure 6b the improved diagram of the SDOF system is plotted, where the time of its response is scaled based on relation (20), attaining a better match with the response of the prototype.

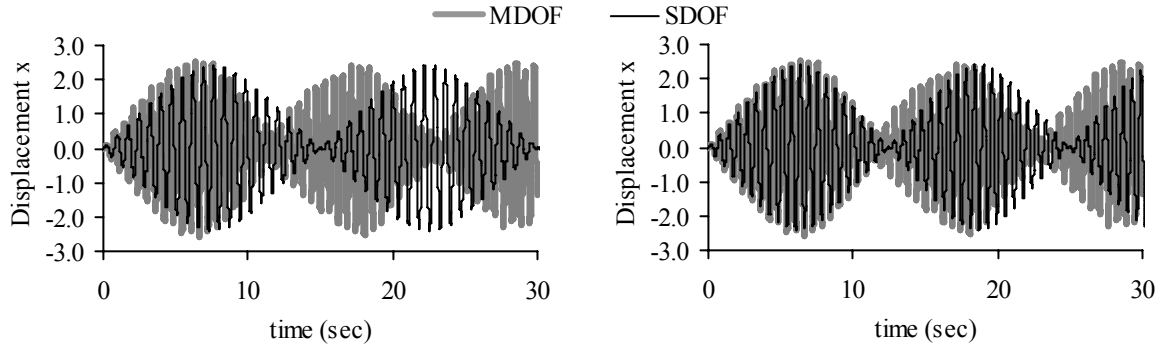

(a) (b)

Figure 6: Time-history response diagrams for $P_p(t)=(1\text{kN})\cos(\omega_p t)$ and $P_m(t)=(169\text{kN})\cos(\omega_m t)$
(a) without time scale (b) with time scale for the model

Similar diagrams are plotted in Figure 7 for the case of small loading frequencies and in Figure 8 for loading frequency larger than the eigenfrequency. In all cases, the proposed transformation of time provides improved accuracy regarding the vibration period.

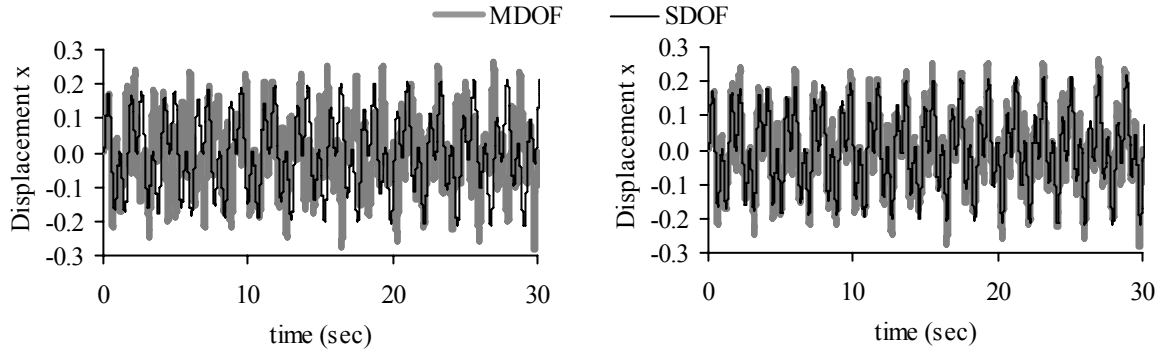

(a) (b)

Figure 7: Time-history response diagrams for $P_p(t)=(1kN)\cos(0.33\cdot\omega_p t)$ and $P_m(t)=(169kN)\cos(0.33\cdot\omega_m t)$ (a) without time scale (b) with time scale for the model

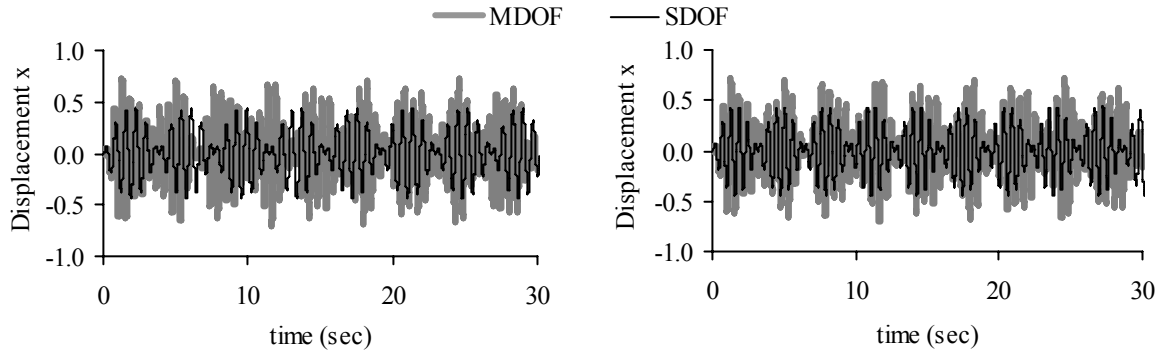

(a) (b)

Figure 8: Time-history response diagrams for $P_p(t)=(1kN)\cos(1.2\cdot\omega_p t)$ and $P_m(t)=(169kN)\cos(1.2\cdot\omega_m t)$ (a) without time scale (b) with time scale for the model

Further, it is noted that structural damping influences the dynamic response of the associated system, affecting significantly the amplitude of the oscillations. In this regard, based on the simulations performed in the current research effort, an improved similarity relation of the damping ratio between the prototype and the model is suggested. This introduction provides with enhanced accuracy regarding the model and the prototype reliability statistics. The new similarity relation proposed herein is given as:

$$\zeta_m = \zeta_p \sqrt[4]{\frac{N_m+1}{N_p+1}} \tag{21}$$

In [2] the response curves for both systems at steady state were compared in fundamental and superharmonic resonant conditions, considering $\zeta_p=\zeta_m=2\%$, and achieving a good accuracy. According to similarity relation (21), the damping ratio equal to $\zeta_p=2\%$ assumed for the prototype corresponds to $\zeta_m=1\%$ for the model, thus, Eq. (1) becomes:

$$\ddot{x} + (0.164\,\mathrm{sec}^{-1})\dot{x} + (8.22\,\mathrm{sec}^{-1})^2 x + (2.64\,\mathrm{sec}^{-2}\,\mathrm{m}^{-2})x^3 = (6.62\,\mathrm{m/sec}^2)\cos\Omega_m t \qquad (22)$$

In what follows, the response diagrams presented in [2] are re-plotted based on the new damping ratio for the model, in an attempt to quantify the influence of the new similarity relation with respect to previously published work of the authors. In this regard, in Figure 9 the response diagram under fundamental resonance presented in [2] is compared with the equivalent one which takes into account ζ_m=1%. It is shown that adopting the new damping ratio the steady-state response of the SDOF model does not alter significantly.

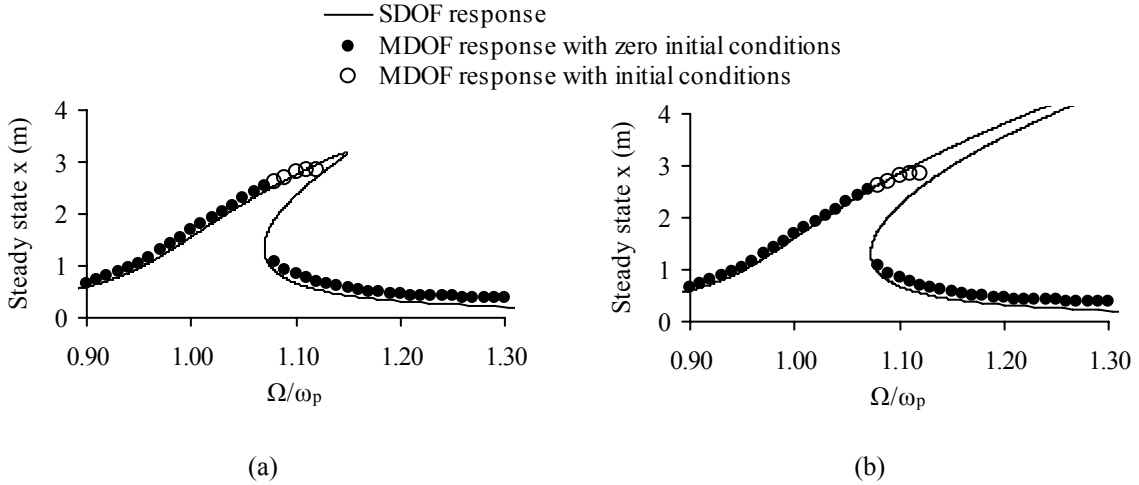

Figure 9: Fundamental resonance: response curve of the MDOF prototype for load amplitude $(P_0)_p$=1.30kN with (a) ζ_m=0.02 (from [2]), (b) ζ_m=0.01

In Figure 10 a time-history diagram of the response under fundamental resonance is plotted, considering both damping ratios for the SDOF cable net. It is observed that changing the damping ratio of the model, the accuracy of the dimension reduction method remains acceptable.

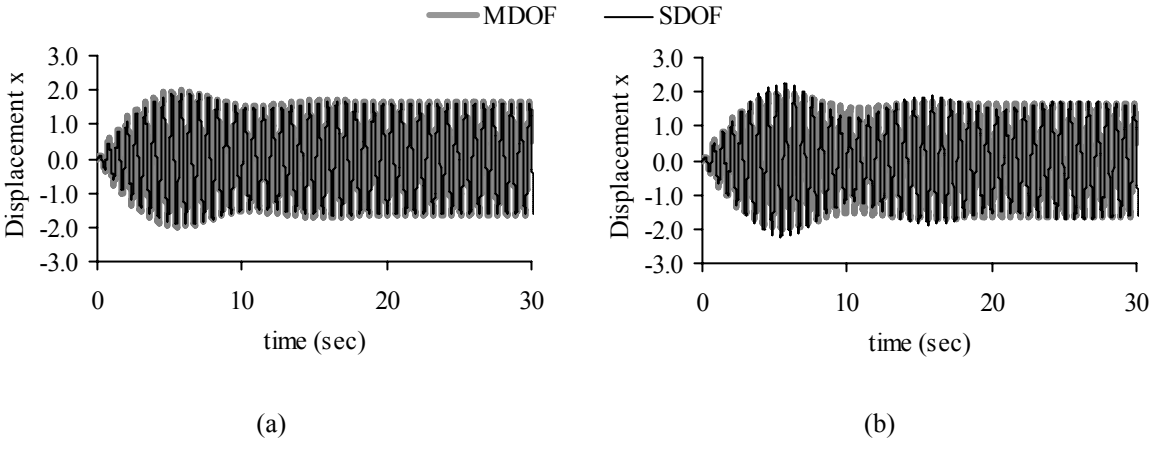

Figure 10: Time-history response diagrams for $P_p(t)=(1.30\text{kN})\cos(\omega_p t)$ and $P_m(t)=(219.7\text{kN})\cos(\omega_m t)$: with (a) ζ_m=0.02, (b) ζ_m=0.01

In Figure 11 the response diagrams at steady state under superharmonic resonance are illustrated, while Figure 12 shows the time-history diagrams for a frequency smaller than the eigenfrequencies of the systems. In those Figures both damping ratios are considered for the

model. It can be readily seen that the different values of the ratio of critical damping do not affect the accuracy of the method significantly.

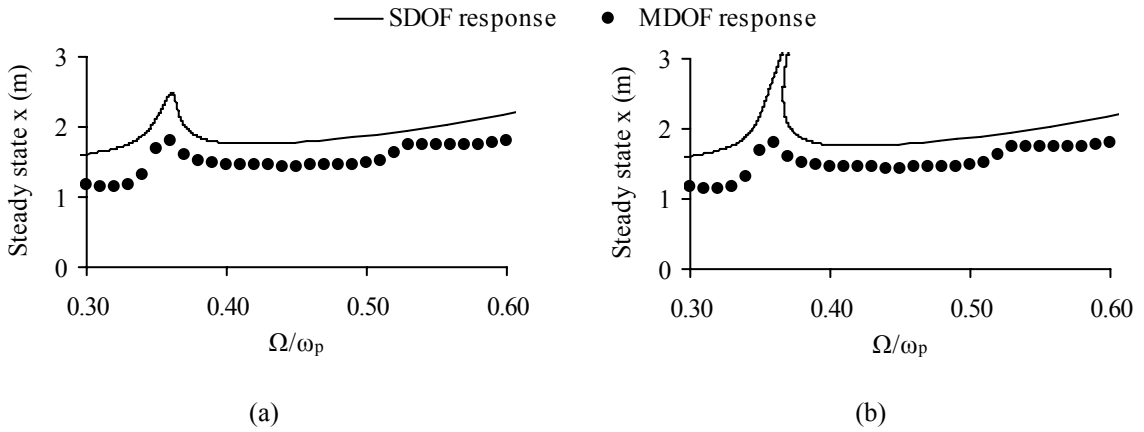

Figure 11: Superharmonic resonance: response curve of the MDOF prototype for load amplitude $(P_0)_p$=14kN with (a) ζ_m=0.02 (from [2]), (b) ζ_m=0.01

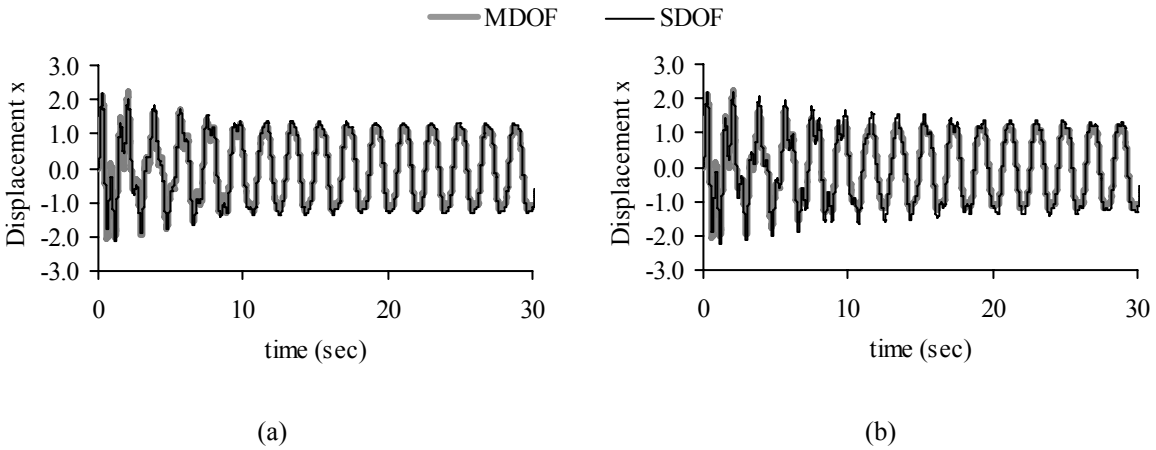

Figure 12: Time-history response diagrams for $P_p(t)=(14kN)\cos(0.33\cdot\omega_p t)$ and $P_m(t)=(2366kN)\sin(0.33\cdot\omega_m t)$ with (a) ζ_m=0.02, (b) ζ_m=0.01

Finally, an additional similarity relation is provided here for the stochastic excitation w(t). Focusing on Eq. (1) each generated realization of the excitation stochastic process w(t) used for exciting the model is transformed into the corresponding one of the prototype, or vice versa, taking into account the similarity relations (3) and (8). Thus,

$$w(t) = \frac{P_m(t)}{M_m} = \frac{P_p(t)}{M_p} \Rightarrow P_p(t) = w(t)M_p \tag{23}$$

4 STOCHASTIC EXCITATION AND THE NUMERICAL PATH INTEGRAL APPROACH

4.1 Introduction

Structural systems are often subject to excitations such as seismic motions, winds, and ocean waves, which can be most realistically described as stochastic processes. Since the pio-

neering work by Caughey and Stumpf [17] several attempts have focused on determining response statistics of linear and nonlinear systems under stochastic excitation (e.g. [18], [19]).

A sustained challenge in the area of stochastic dynamics is the determination of the probability that the system response stays within a prescribed domain within a specified time interval. Such a reliability-based analysis can be beneficial in terms of safety or risk assessment. An alternative equivalent definition of the aforementioned challenge, known as the first-passage problem, is the evaluation of the probability that the response of the system reaches, and possibly crosses, a predetermined level for the first time.

One of the promising frameworks for addressing the stochastic response determination and the first-passage problem challenges is related to the concept of the Wiener Path Integral (WPI). The concept of the functional path integral was introduced by Wiener [20], and was re-invented in a different form by Feynman [21] in the field of theoretical physics. Recently, a Wiener Path Integral based approximate analytical technique was developed by Kougioumtzoglou and Spanos [22] to address certain challenges in the area of engineering dynamics.

Further, numerical versions of the WPI solution have been employed in engineering applications to derive response and reliability statistics of nonlinear systems (e.g. [23] – [25]). Most of the developed numerical path integral approaches constitute, in essence, a discrete version of the well-known Chapman-Kolmogorov (C-K) equation which is associated with Markov processes (e.g. [26]). The basic characteristic of this approach is that the evolution of the response probability density function (PDF) is computed in short time steps, assuming a Gaussian form for the conditional response PDF. It was Wehner and Wolfer [27] who first addressed certain numerical aspects of the approach and established it as a robust numerical tool.

Recently, a generalized numerical path integral approach (NPI) has been developed by one of the authors [9] for determining response and first-passage statistics of nonlinear oscillators subject to evolutionary broad-band stochastic excitation. The NPI approach is utilized in the following to determine the non-stationary response amplitude PDF and the survival probability of the Duffing oscillator of Eq. (1) under Gaussian white noise excitation.

4.2 Mathematical formulation elements

In the following, a brief overview of the NPI approach proposed in [9] is included for completeness. In this regard, consider a nonlinear single-degree-of-freedom system whose motion is governed by the differential equation:

$$\ddot{x} + \beta\dot{x} + z(t, x, \dot{x}) = w(t) \tag{24}$$

where a dot over a variable denotes differentiation with respect to time t; $z(t, x, \dot{x})$ is the restoring force which can be either hysteretic or depend only on the instantaneous values of x and $\dot{x}$; β is a linear damping coefficient; and w(t) represents a Gaussian, zero-mean non-stationary stochastic process possessing an evolutionary broad-band power spectrum, $S(\omega, t)$.

Considering next the case of a lightly damped system, it can be argued that the nonlinear oscillator of Eq. (24) exhibits a pseudo-harmonic behaviour described by the equations:

$$x(t)=A(t)\cos[\omega(A)t+\varphi(t)] \tag{25}$$

and

$$\dot{x}(t) = -\omega(A)A(t)\sin[\omega(A)t + \varphi(t)] \tag{26}$$

where the response amplitude envelope A is a slowly varying function with respect to time and, thus, can be treated as a constant over one cycle of oscillation.

Further, following a statistical linearization approach discussed in [18] and [28], a linearized counterpart of Eq. (24) is:

$$\ddot{x} + \beta(A)\dot{x} + \omega^2(A)x = w(t) \tag{27}$$

For the special case of the Duffing oscillator (see [9] for a more detailed presentation), namely for

$$z(t, x, \dot{x}) = \omega_0^2 x + \varepsilon\omega_0^2 x^3 \tag{28}$$

(ε being a nonlinearity magnitude parameter) the equivalent damping element and the natural frequency are given by the expressions

$$\beta(A)=\beta \tag{29}$$

and

$$\omega^2(A) = \omega_0^2\left(1 + \frac{3}{4}\varepsilon A^2\right) \tag{30}$$

Taking into account Eq. (25) and Eq. (26), the amplitude A can be expressed in the form:

$$A^2(t) = x^2(t)\left(\frac{\dot{x}(t)}{\omega(A)}\right)^2 \tag{31}$$

Relying once more on the assumption of light damping, simplification of Eq. (27) is possible by further application of stochastic averaging (e.g. [18], [29]). This yields the Ito stochastic differential equation [26]:

$$\dot{A} = K_1(A,t) + K_2(A,t)\eta(t) \tag{32}$$

where

$$K_1(A,t) = -\frac{1}{2}\beta(A)A(t) + \frac{\pi S(\omega(A),t)}{2A(t)\omega^2(A)} \tag{33}$$

and

$$K_2(A,t) = \frac{\sqrt{\pi S(\omega(A),t)}}{\omega(A)} \tag{34}$$

which governs approximately the evolution in time of the amplitude A(t). In Eq. (32), $\eta(t)$ is a zero mean and delta correlated Gaussian process of intensity one, i.e., $E(\eta(t))=0$; and $E(\eta(t)\eta(t+\tau))=\delta(\tau)$, with $\delta(\tau)$ being the Dirac delta function. The Fokker-Planck (F-P) equation which corresponds to Eq. (32) takes the form (e.g. [26])

$$\frac{\partial}{\partial t}p(A, t+\Delta t \mid A', t) = -\frac{\partial}{\partial A}[K_1(A,t)p(A, t+\Delta t \mid A', t)] + \frac{1}{2}\frac{\partial^2}{\partial A^2}[K_2^2(A,t)p(A, t+\Delta t \mid A', t)] \tag{35}$$

The significance of Eq. (32) relates to the fact that the amplitude A(t) is decoupled from the phase $\varphi(t)$. Thus, it is feasible to model the amplitude process A(t) as a one-dimensional Markov diffusion process (e.g. [26], [30]). Hence, the C-K equation

$$p(A,t+2\Delta t \mid A'',t)=\int_0^{\infty} p(A,t+2\Delta t \mid A',t+\Delta t)p(A',t+\Delta t \mid A'',t)dA' \tag{36}$$

is satisfied, where $p(A,t+\Delta t \mid A',t)$ represents the conditional PDF of the response amplitude process. Note that the NPI approach proposed in [9] involves the numerical evaluation of one integral only in Eq. (36); this is due to the fact that a stochastic averaging treatment has been utilized to reduce the original second-order SDE Eq. (24) to a first-order SDE of the form of Eq. (32). Although it can be argued that the stochastic averaging treatment introduces additional approximations to the problem, it renders the NPI approach significantly less computationally demanding than alternative NPI approaches applied directly to Eq. (24) (e.g. [23]). In the latter case, Eq. (36) involves a double integral, which increases considerably the computational cost.

Further, the evaluation of the reliability function $R_B(T)$ is possible (e.g. [31]). This is defined as the probability that the system response amplitude stays below the threshold B over the time interval $[t_0,T]$. Specifically, considering the time interval $[t_0,T]$ discretized so that $t_j=t_0+j\Delta t$, $j=0,1,\ldots,n$ and $\Delta t=(T-t_0)/(n)$, and assuming an initial PDF $p(A_0,t_0)$, the reliability function $R_B(t_j)$ becomes

$$R_B(t_j)=\int_0^{B}\int_0^{\infty} p(A_j,t_j \mid A_{j-1},t_{j-1})\ldots\int_0^{B}\int_0^{\infty} p(A_1,t_1 \mid A_0,t_0)dA_1\ldots dA_j \tag{37}$$

It can be readily seen that knowledge of the conditional PDF suffices to evaluate Eq. (37) using Eq. (36). The interesting feature of the F-P Eq. (35) is that the conditional PDF $p(A,t+\Delta t \mid A',t)$, often called short-time propagator, has been shown to follow a Gaussian distribution (e.g. [32]) of the form

$$p(A,t+\Delta t \mid A',t)=\frac{1}{\sqrt{2\pi K_2^2(A',t)\Delta t}}\exp\left(-\frac{(A-A'-K_1(A',t)\Delta t)^2}{2K_2^2(A',t)\Delta t}\right) \tag{38}$$

5 NUMERICAL EXAMPLES

In this section the Duffing oscillator of Eq. (1), or equivalently of Eq. (24) taking into account Eq. (28), is considered with a nonlinearity parameter $\varepsilon=0.039$ subject to Gaussian white noise excitation with a power spectrum $S(\omega,t)=S_0$. The value of parameter ε is computed so that there is an equivalence between Eq. (1) and Eqs. (24) and (28). In the numerical examples, three values of S_0 are chosen, namely $5m^2{\cdot}sec/rad$, $7.5m^2{\cdot}sec/rad$ and $10m^2{\cdot}sec/rad$, corresponding to maximum loading amplitudes $(P_0)_p$ equal to $0.57kN/m^2$, $0.70kN/m^2$ and $0.81kN/m^2$, respectively. These are realistic values of a dynamic load, considering that for an actual project of a similar cable net, the roof of Peace and Friendship Stadium in Greece [33], the wind load of the final design was $1.10kN/m^2$. Further, a total time duration $t_{p,total}=30sec$ is considered for all analyses of the prototype, for which, both systems reach steady-state response. This time duration is transformed for the model according to the inverse relation of (20):

$$t_{m,total}=t_{p,total}\left(\frac{N_p+1}{N_m+1}\right)^{0.07}=35.90\,\text{sec} \tag{39}$$

As far as numerical implementation issues and convergence criteria are concerned for the NPI approach, an extended discussion of conditions to be satisfied for the values of the time increment and the grid size is provided in [27]. Further, the initial distribution chosen for the response amplitude PDF is the Dirac delta function, namely $p(A,t=0)=\delta(A)$, assuming the system is initially at rest. For the Monte Carlo simulations of the prototype MDOF system an ensemble of 500 realizations is used. Although it is recognised that this number is quite small for capturing detailed system response PDF characteristics, it is noted that the main aim of the approach relates to a preliminary (reliability-based) system design. In this regard, the number of realizations is deemed adequate for estimating the general features of the MDOF system non-stationary response PDF.

5.1 Non-stationary response amplitude PDF

In Figure 13 the non-stationary response amplitude PDFs for the prototype and the model are shown for $S_0=5m^2$·sec/rad. It is noted that the proposed dimension reduction approach based on the NPI performs satisfactorily in capturing the essential characteristics of the MDOF system non-stationary response PDF. Similarly, in Figures 14 and 15 the non-stationary response amplitude PDFs for the prototype and the model are shown for $S_0=7.5m^2$·sec/rad and for $S_0=10m^2$·sec/rad, respectively.

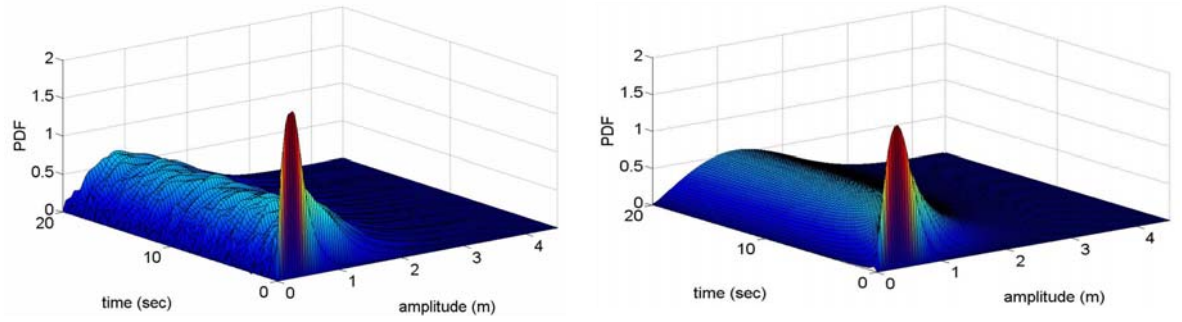

(a) (b)

Figure 13: Non-stationary response amplitude PDF for $S_0=5m^2$·sec/rad: (a) MDOF (MCS) and (b) SDOF (NPI)

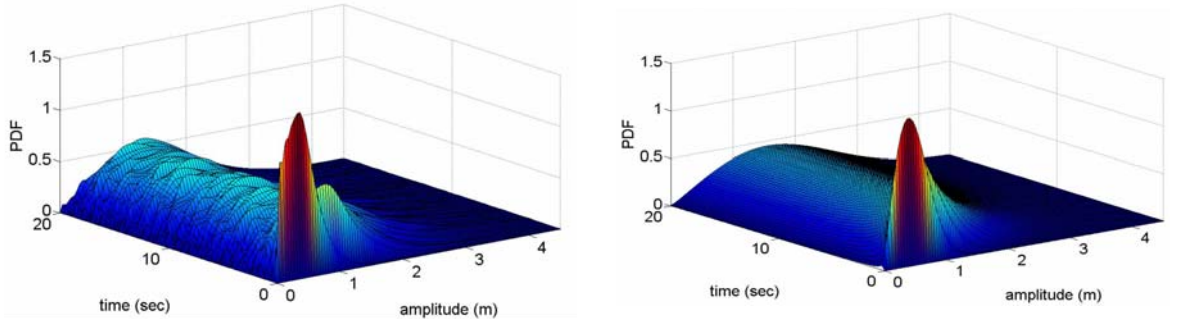

(a) (b)

Figure 14: Non-stationary response amplitude PDF for $S_0=7.5m^2$·sec/rad: (a) MDOF (MCS) and (b) SDOF (NPI)

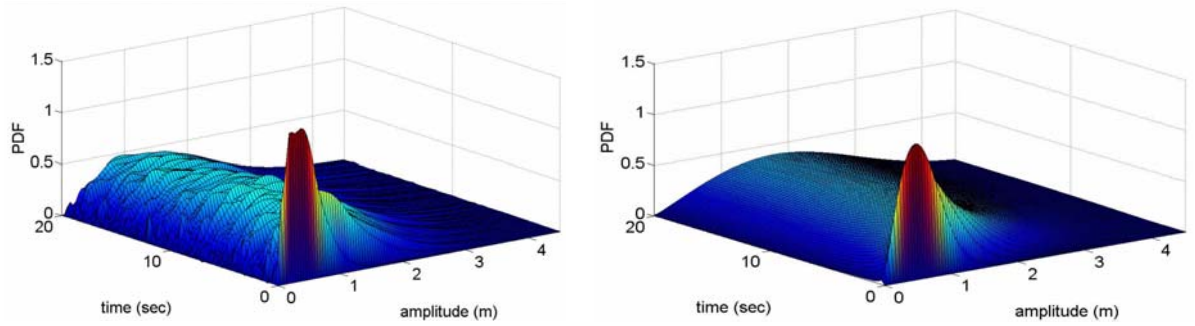

(a) (b)

Figure 15: Non-stationary response amplitude PDF for S_0=10m^2·sec/rad: (a) MDOF (MCS) and (b) SDOF (NPI)

The comparison between the diagrams of the SDOF model and the MDOF system shows a satisfactory level of accuracy. Thus, the proposed dimension reduction method based on the NPI approach can be used at a preliminary design stage to estimate the probability for the MDOF cable net to reach a certain value of displacement at a given time, during transient or steady state response, using the equivalent SDOF model.

5.2 Reliability function

The failure barrier level is set to B=3.975m accounting for a maximum permissible cable stress as explained in section 3.2. All analyses performed with ADINA for the prototype have a material law for which the tension branch arrives at the yield stress, as shown in Figure 3. As mentioned in section 5, the total time is 30sec for the prototype and 35.90sec for the model, while the results of the latter are time scaled, according to the inverse relation of Eq. (20), in order to match the time for the prototype.

Figure 16a depicts the reliability function (survival probability) for S_0=7.5m^2 sec/rad. The maximum difference between the MDOF prototype and the SDOF model is found to be approximately 1%. Similarly, in Figure 16b the reliability functions are plotted for S_0=10m^2·sec/rad, which corresponds to a larger excitation magnitude; thus, causing naturally more failure events for both systems. The maximum difference between the prototype and the model, regarding the calculation of R(t) is found to be approximately 16%. In both diagrams, the proposed dimension reduction approach based on the NPI demonstrates a satisfactory level of accuracy.

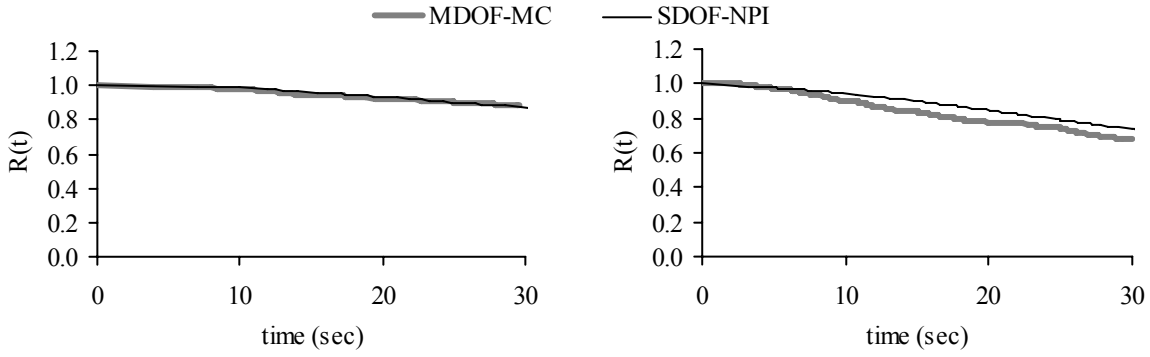

(a) (b)

Figure 16: Reliability function R(t) vs time for (a) S_0=7.5m^2·sec/rad and (b) S_0=10m^2·sec/rad

Based on those results it can be concluded that the proposed dimension reduction methodology based on a NPI approach is capable of predicting with satisfactory accuracy the reliability of a large cable net, circumventing the computationally prohibitive in many cases MCS based nonlinear dynamic analyses of the original MDOF system.

6 CONCLUSIONS

In this paper, a dimension reduction approach based on a recently proposed NPI technique introduced in [9] has been developed for determining the non-stationary response amplitude PDF and the survival probability of a MDOF symmetric cable net system with fixed cable ends under Gaussian white noise excitation. Specifically, the concept of similarity relationships, as used in [2], has been employed to reduce the original MDOF system to a SDOF nonlinear oscillator of the Duffing kind. Next, a NPI based approach in conjunction with a stochastic averaging treatment has been utilized to determine the non-stationary response amplitude PDF and the survival probability of the Duffing oscillator.

It has been shown that the proposed dimension reduction approach succeeds in capturing the essential characteristics of the original MDOF system response behaviour in an average manner. In this regard, relatively accurate cable tensile failure probability estimates have been derived at a minimum computational cost for a selected illustrative numerical example; thus, rendering the herein proposed dimension reduction approach a strong candidate for preliminary reliability based design of such structures. Specifically, it can be used potentially for the preliminary design of such structural systems by appropriately choosing the geometry of the cable net, the cable diameter and initial pretension so that failure probability values prescribed by relevant code provisions are satisfied. Regarding future work, more sophisticated excitation power spectrum forms modelling wind loads can be used; this is especially important considering the fact that wind loads are the prevalent dynamic loads which threaten the safety of such structures.

REFERENCES

[1] I. Vassilopoulou, *Nonlinear dynamic response and design of cable nets*, Doctoral Thesis. National Technical University of Athens, Greece, 2011.

[2] I. Vassilopoulou and C. J. Gantes, Nonlinear dynamic behaviour of a saddle form cable net modeled by an equivalent SDOF cable net. M. Papadrakakis, M. Fragiadakis, V. Plevris eds. *3rd ECCOMAS Thematic Conference on Computational Methods in Structural Dynamics and Earthquake Engineering – (COMPDYN 2011)*, Corfu, Greece, May 25-28, 2011.

[3] J.S. Gero, The behaviour of cable network structures. *Structures Report SR8*, University of Sydney, Australia, 1975.

[4] J.S. Gero, The preliminary design of cable network structures. *Structures Report SR9*, University of Sydney, Australia, 1975.

[5] I. Vassilopoulou and C.J. Gantes, Behaviour and preliminary analysis of cable net structures with elastic supports. D.E. Beskos, D.L. Karabalis, A.N. Kounadis eds. *4th National Conference on Metal Structures*, Patras, Greece, **2**, 517-525, May 24-25, 2002.

[6] I. Vassilopoulou and C.J. Gantes, Behavior, analysis and design of cable networks anchored to a flexible edge ring. *IASS Symposium on Shell and Spatial Structures from Models to Realization*, Montpellier, France, Extended Abstract, 212-213, 2004.

[7] I. Vassilopoulou and C.J. Gantes, Cable nets with elastically deformable edge ring. *International Journal of Space Structures*, **20**, 15-34, 2005.

[8] I. Vassilopoulou and C.J. Gantes, Similarity relations for nonlinear dynamic oscillations of a cable net. M. Papadrakakis, D.C Charmpis, N.D. Lagaros, Y. Tsompanakis eds. *1st ECCOMAS Thematic Conference on Computational Methods in Structural Dynamics and Earthquake Engineering (COMPDYN 2007)*, Rethymno, Crete, Greece, abstract 373, June 13-16, 2007.

[9] I. A. Kougioumtzoglou and P. D. Spanos, Response and first-passage statistics of nonlinear oscillators via a numerical path integral approach, *ASCE Journal of Engineering Mechanics*, doi:10.1061/(ASCE)EM.1943-7889.0000564, 2012, (In Press).

[10] A. K. Chopra, *Dynamics of structures, theory and applications to earthquake engineering*, Prentice Hall International, Inc., U.S.A., 1995.

[11] ADINA (Automatic Dynamic Incremental Nonlinear Analysis) v8.4, *ADINA User interface command reference manual, Vol. I: ADINA Solids & Structures model definition*. ADINA R & D, Inc., U.S.A., 2006.

[12] ADINA (Automatic Dynamic Incremental Nonlinear Analysis) v8.4, *Theory and modeling guide, Vol. I: ADINA Solids & Structures*. ADINA R & D, Inc., U.S.A., 2006.

[13] I. Vassilopoulou and C.J. Gantes, Nonlinear dynamic phenomena in a SDOF model of cable net. *Archive of Applied Mechanics*, **82**, 1689-1703, 2012.

[14] A. Nayfeh and D.T. Mook, *Nonlinear Oscillations*. John Wiley & Sons, Inc. U.S.A., 1979.

[15] H. A. Buchholdt, *An introduction to cable roof structures*. Thomas Telford, 2nd Edition, Great Britain, 1999.

[16] MATLAB, *The language of technical computing*. v.7.9.0.529 (R2009b), The MathWorks, Inc., U.S.A., 2009.

[17] T. K. Caughey and H. J. Stumpf, Transient response of a dynamic system under random excitation. *Journal of Applied Mechanics*, **27**, 563-566, 1961.

[18] I. A. Kougioumtzoglou and P. D. Spanos, An approximate approach for nonlinear system response determination under evolutionary stochastic excitation. *Current Science, Indian Academy of Sciences*, **97**, 1203-1211, 2009.

[19] P. D. Spanos and I. A. Kougioumtzoglou, Harmonic wavelets based statistical linearization for response evolutionary power spectrum determination. *Probabilistic Engineering Mechanics*, **27**, 57-68, 2012.

[20] N. Wiener, Generalized harmonic analysis. *Acta Mathematica*, **55**, 117-258, 1930.

[21] R. P. Feynman, Space-time approach to non-relativistic quantum mechanics. *Reviews of Modern Physics*, **20**, 367-387, 1948.

[22] I. A. Kougioumtzoglou and P. D. Spanos, An analytical Wiener path integral technique for non-stationary response determination of nonlinear oscillators. *Probabilistic Engineering Mechanics*, **28**, 125-131, 2012.

[23] A. Naess and J. M. Johnsen, Response statistics of nonlinear, compliant offshore structures by the path integral solution method. *Probabilistic Engineering Mechanics*, **8**, 91-106, 1993.

[24] A. Naess, D. Iourtchenko and O. Batsevych, Reliability of systems with randomly varying parameters by the path integration method. *Probabilistic Engineering Mechanics*, **26**, 5-9, 2011.

[25] A. Pirrotta and R. Santoro, Probabilistic response of nonlinear systems under combined normal and Poisson white noise via path integral method. *Probabilistic Engineering Mechanics*, **26**, 26-32, 2011.

[26] C. W. Gardiner, *Handbook for Stochastic Methods for Physics, Chemistry and the Natural Sciences*. Springer-Verlag, Berlin, Heidelberg, New York, 1985.

[27] M. F. Wehner and W. G. Wolfer, Numerical evaluation of path-integral solutions to Fokker-Planck equations. *Physical Review A*, **27**, 2663-2670, 1983.

[28] J. B. Roberts and P. D. Spanos, *Random Vibration and Statistical Linearization*. New York: Dover Publications, 2003.

[29] J. B. Roberts and P. D. Spanos, Stochastic Averaging: an approximate method of solving random vibration problems. *International Journal of Non-Linear Mechanics*, **21**, 111-134, 1986.

[30] T. T. Soong and M. Grigoriu, *Random Vibration of Mechanical and Structural Systems*. Prentice Hall, New Jersey, 1993.

[31] D. Iourtchenko, E. Mo and A. Naess, Reliability of strongly nonlinear single degree of freedom dynamic systems by the path integration method. *Journal of Applied Mechanics*, **75**, 061016-1-061016-8, 2008.

[32] H. Dekker, Time-local Gaussian processes, path integrals and nonequilibrium nonlinear diffusion", *Physica*, **85A**, 363-373, 1976.

[33] R. Alessi, D. Bairaktaris, F. Caridakis, M. Majowiecki and F. Zoulas, The roof structures of the new sports arena in Athens. *World Congress on Shell and Spatial Structures*, Spain, 6.107-6.123, 1979.